International Journal of Heat and Mass Transfer 61 (2013) 419–424

Contents lists available at SciVerse ScienceDirect

International Journal of Heat and Mass Transfer

journal homepage: www.elsevier.com/locate/ijhmt

Effect of oscillatory EHD on the heat transfer performance of a flat plate

Wen-Junn Sheu [a], Jen-Jei Hsiao [a], Chi-Chuan Wang [b,*]

[a] Department of Power Mechanical Engineering, National Tsing Hua University, Hsinchu 300, Taiwan
[b] Department of Mechanical Engineering, National Chiao Tung University, Hsinchu 300, Taiwan

ARTICLE INFO

Article history:
Received 29 August 2012
Received in revised form 5 February 2013
Accepted 8 February 2013
Available online 5 March 2013

Keywords:
Electrohydrodynamics
Ionic wind
Oscillatory EHD
Enhanced convection

ABSTRACT

The present study investigates the effect of oscillatory EHD on the heat transfer performance of a flat plate. A needle type electrode with positive polarity is used to generate ionic wind with applied voltage ranging from 4 to 9.5 kV. The wave forms of the input voltage are either steady or stepped and the frequency ranges from 0.5 to 2 Hz with the separation distance between the electrode and the test plate being 5 and 15 mm, respectively. It is found that at the same applied voltage, the heat transfer performance subject to the oscillatory EHD is always inferior to that of the steady EHD for all frequencies. A parabolic dependence of the ionic current with the supplied voltage is seen under steady EHD operation. However, the ionic current vs. supplied voltage shows a rather linear dependence pertaining to the oscillatory EHD. For a smaller separation distance of 5 mm, the heat transfer performance for $f = 0.5$ Hz is slightly higher than that of $f = 2$ Hz. However, the trend is reversed when the separation distance is increased to 15 mm.

1. Introduction

The presence of a high electric field between a discharged and a grounded electrode bring about an air motion which is normally regarded as the ionic wind. The pioneer studies employing the ionic wind as a cooling method can be dated back to late 1960s [1,2] and since then the use of electrohydrodynamics (EHD) for heat transfer augmentation applicable for single-phase or two-phase heat transfer had been reported considerably. An early review by Allen and Karayiannis [3] had outlined the basic enhancement mechanisms and a comprehensive review of past work. Recently, fan-less heat transfer augmentation such as cooling of LEDs under natural convection gains much attention. This is because the major concern of noise. In common implementation of heat transfer augmentation for LED cooling, passive methods incorporating natural convection heat sinks such as plate fin, pin fin and radial fin (e.g. [4–6]) are mostly adopted. Active methods such as microjet array cooling, liquid-cooling, thermoelectric cooler, and oscillating heat pipes are also feasible techniques that efficiently dissipate heat out of the high power LEDs (e.g. [7–10]). Despite the foregoing active methods show effective heat removal in high power LEDs, concerns of noise and vibration resulting from the moving parts of these active methods remain. Therefore, rather than using mechanical devices to promote cooling, ionic wind featuring the benefit of forced convection but free of noise concerns is one of the potential candidates. This would certainly simplify the design and increase the reliability of the cooling module for LED devices due to the lack of moving parts.

There had been intensive studies in association with the EHD applicable for heat transfer augmentation subject to natural convection (e.g. [11–22]). These previous efforts investigated heat transfer augmentation in various configurations and electrode arrangements under steady EHD operation. It appeared that no efforts had been made concerning the influence of oscillatory electric field on the heat transfer performance. In this regard, it is the objective of this study to provide some preliminary results about the influence of oscillatory electric field on the heat transfer performance pertaining to natural convection of a plate heat sink.

2. Experimental setup

The schematic of the test facility is shown in Fig. 1(a). It contains a functional generator (Tectronix AFG 3022), a high voltage power supply (positive polarity, up to 10 kV, from YOU-SHANG Technical Corp.), a power meter (DM-1250), an acrylic housing, and the test section. The test plate is an aluminum alloy with an effective thermal conductivity of 175 $W\,m^{-1}\,K^{-1}$. The size of the test section is 45 mm (W) × 45 mm (L) × 2 mm (H). A Kapton heater is adhered to the bottom of the heat sink with a high thermal conductivity grease ($k = 2.1\ W\,m^{-1}\,K^{-1}$). The heater is of the same size as the base plate for removing the spreading resistance. In addition, a VIP (vacuum insulation panel) insulation plate with a

* Corresponding author. Address: E474, 1001 University Road, Hsinchu 300, Taiwan. Tel.: +886 3 5712121x55105; fax: +886 3 5720634.
E-mail addresses: ccwang@mail.nctu.edu.tw, ccwang@hotmail.com (C.-C. Wang).

0017-9310/$ - see front matter © 2013 Elsevier Ltd. All rights reserved.
http://dx.doi.org/10.1016/j.ijheatmasstransfer.2013.02.026

Nomenclature

A	surface area, m^2
E_r	enhancement index for natural convection, dimensionless
f	frequency, Hz
H	height, mm
i	corona current, μA
h	heat transfer coefficient, $W\,m^{-2}\,K^{-1}$
$\bar{h}_{ehd}$	average heat transfer coefficient under EHD operation, $W\,m^{-2}\,K^{-1}$
$\bar{h}_{nc}$	average heat transfer coefficient under natural convection, $W\,m^{-2}\,K^{-1}$
k	thermal conductivity, $W\,m^{-1}\,K^{-1}$
L	length, mm
P	power, W
Q_t	total heat transfer rate, W
Q_f	heat supplied to the heat sink, W
Q_l	heat loss from the bakelite, W
R	electrical resistance, Ω
T	temperature, °C
T_b	surface temperature of the base plate, °C
T_∞	ambient temperature, °C
$T_{ins,c1}$	measured temperature at the top of the bakelite, °C
$T_{ins,c2}$	measured temperature at the bottom of the bakelite, °C
ΔT	temperature difference between LED and ambient, °C
V	voltage, V

very low thermal conductivity of 0.004 $W\,m^{-1}\,K^{-1}$ is placed beneath the heater to reduce the heat loss. The heater is powered by a DC power supply. The needle electrode is made of tungsten with a radius of 3 μm at the tip of the needle. The electrode is connected to a high voltage generator with the heat sink being grounded. The vertical separation of the electrode to the test plate is fixed at 5 mm.

Five T-type thermocouples are equally attached to the base plate of the heat sink to obtain the mean temperature of the base plate (T_b). The thermocouples were pre-calibrated with an accuracy of 0.1 °C. The average temperature is then used to estimate the surface temperature of the heat sink via Fourier's law of conduction. The ambient temperature is normally around 22–25 °C, and the system pressure is around 100 kPa. The measurements of thermocouples are collected via the data acquisition system MX100 from YOKOGAWA.

The high voltage generator is specially made with variable voltages of 0–10 kV. A voltmeter (YFE YF-3120) with an accuracy of 0.8% is bridged across the voltage generator and a microammeter (YOKOGAWA 73203) with a resolution of 0.1 μA is connected between the heat sink and the voltage generator to obtain the applied voltage and the corona current, respectively.

For visualization of the influence of ionic wind, a smoke generator capable of generating water vapor is used. The generated water vapor is directed by a capillary tube with strainghter and is attached to the electrode as shown in Fig. 1(b). The generated smoke is entrained by the supplied EHD flow along the flat plate. A He–Ne laser from Actor-Mate Corp. with a wave length of 532 nm and a maximum output power of 100 mW is used to visualize the generated ionic wind.

3. Data reduction

The total supplied heat input (Q_t) is 3.5 W which can be obtained by the applied voltage and a given resistance of the heater. Notice that a VIP (vacuum insulation panel) is installed below the heater with effective thermal conductivity of 0.004 $W\,m^{-1}\,K^{-1}$, thereby eliminating the major heat loss below the heater. An insulation box made of bakelite with a low thermal conductivity of 0.233 $W\,m^{-1}\,K^{-1}$ is placed beneath the VIP. In addition, a total of four T-type thermocouples are installed inside the bakelite. The measured average temperature in the backlite is then used to estimate the heat loss via Fourier's law of conduction. The heat supplied to the heat sink (Q_f) is thus obtained by subtracting the heat loss from the total power input:

$$Q_t = \frac{V^2}{R} \tag{1}$$

$$Q_l = kA\frac{dT}{dx} = kA\frac{T_{ins,c1} - T_{ins,c2}}{t} \tag{2}$$

$$Q_f = Q_t - Q_l \tag{3}$$

The effective heat transfer coefficient is calculated by Newton's law of cooling:

$$Q_f = \bar{h}A(T_b - T_\infty) \tag{4}$$

The index of the EHD performance is characterized by the enhancement index for natural convection (E_r) which represents the average heat transfer coefficient with EHD divided by that without EHD:

$$E_r = \frac{\bar{h}_{ehd}}{\bar{h}_{nc}} \tag{5}$$

Notice that the subscript *ehd* and *nc* represents test conditions that are conducted under ionic wind and natural convection condition, respectively. The experimental uncertainty is estimated using the uncertainty propagation equation recommended by Kline and McClintock [23]. Normally, a total of 100 samples were taken during the experiment. The calculated uncertainty of heat transfer coefficient varies from 1.74% to 6.15% while the enhancement index for natural convection (E_r) varies from 2.46% to 6.59% with the confidence level of 95%.

4. Results and discussion

The wave forms of the input voltage are either steady or oscillatory (stepped function). The frequency ranges from 0.5 to 2 Hz and the input power is 3.5 W with the separation distance between the electrode and the test plate being 5 and 15 mm, respectively. Fig 2(a) shows the enhancement heat transfer ratio, E_r, vs. applied voltage amid the steady EHD and stepped EHD at a separation distance of 5 mm and Fig. 2(c) depicts the variation of thermal resistance against the supplied voltage. Note that the airflow induced by EHD is inclined to the flat plate. The airflow is not totally downward, it has an axial component that is parallel to the flat plate and is perpendicular to the buoyancy airflow direction. With this component, it distorted the rising airflow considerably and eventually improves the heat transfer performance as shows in Fig. 2(a).The results clearly show that the enhancement ratio under steady EHD operation outperforms those of oscillatory operations. On the other hand, the enhancement ratios for the frequency ranging from 0.5 to 1.5 Hz are comparable whereas E_r for $f = 2$ Hz is apparently lower than those of lower frequencies. In fact, a maximum deviation of 7% in E_r for $f = 2$ Hz is found at a supplied voltage of 4 kV. The results are quite similar to those calculations made by Lai et al. [24] to some extent. Note that Lai et al. [24] conducted

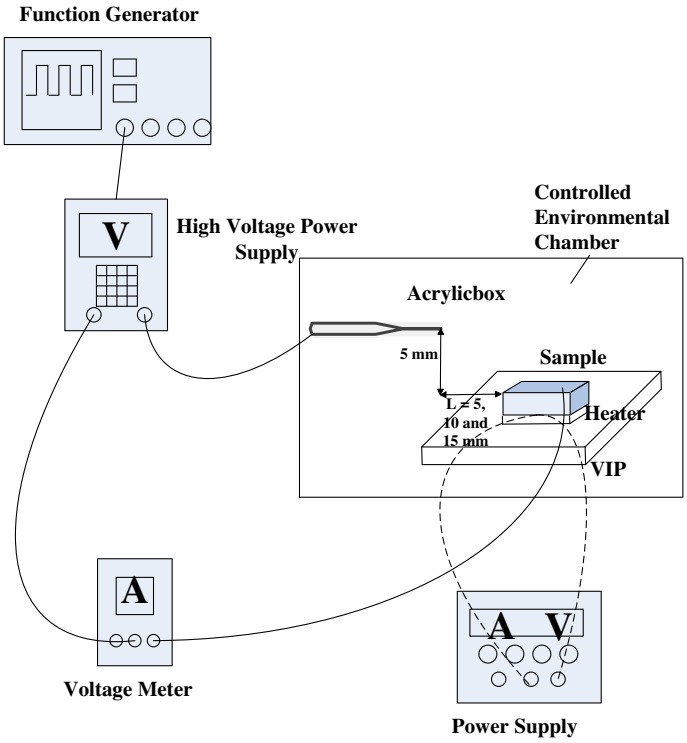

(a) Schematic of the experimental setup for heat transfer measurement.

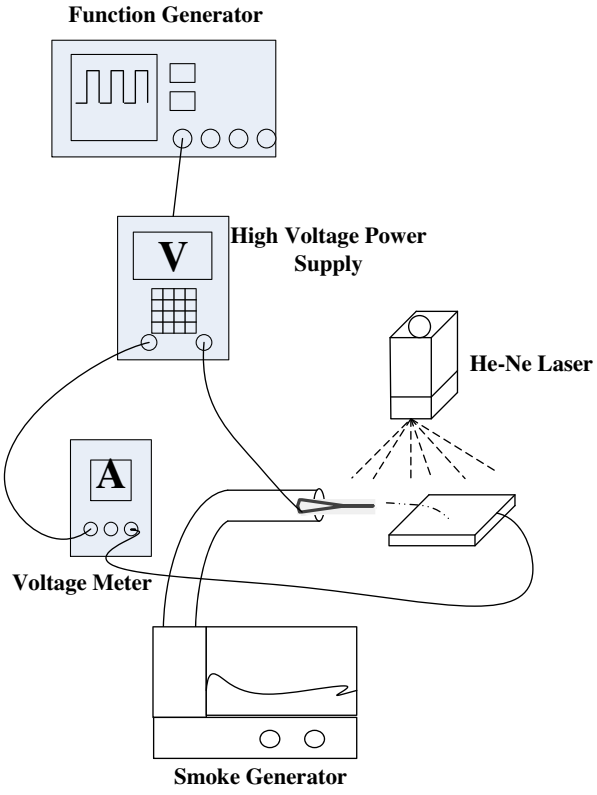

(b) Schematic of the flow visualization setup. (c) Smoke generator

Fig. 1. Schematic of the test facility.

a numerical simulation of the oscillatory EHD flow in a positive wire-plate electrostatic precipitator. Two regimes of oscillation are observed in their simulation. The flow is characterized by a single eddy that is opposed to the wire and oscillates with frequencies between 1.2 and 4.3 Hz. The second regime is characterized by counter rotating eddies that oscillates amid 0.6 and 1.6 Hz. Despite

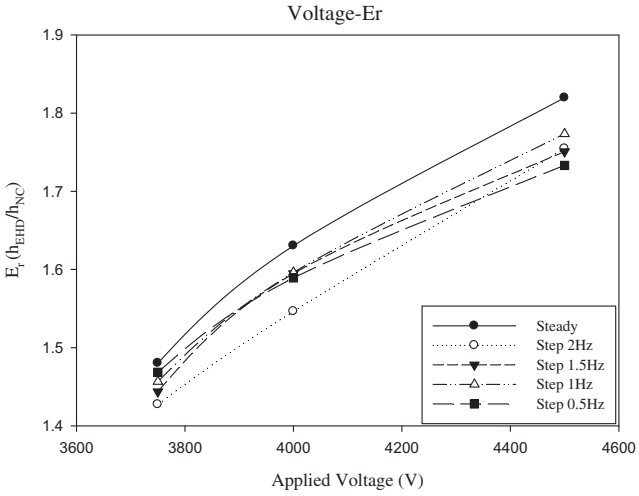

(a) Enhancement index for natural convection vs. applied voltage.

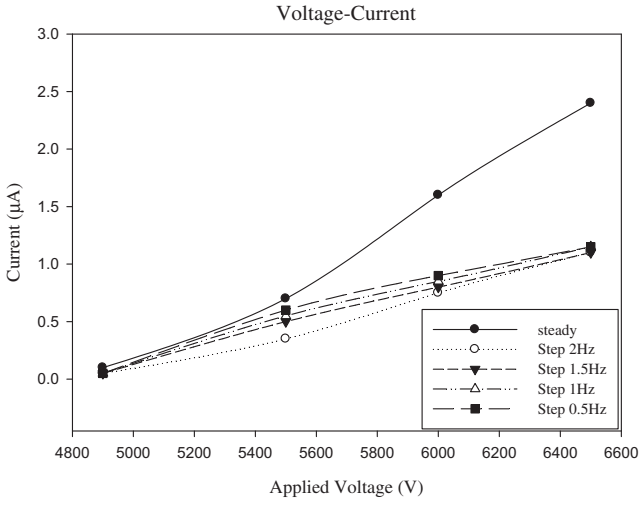

(b) Ionic current vs. applied voltage.

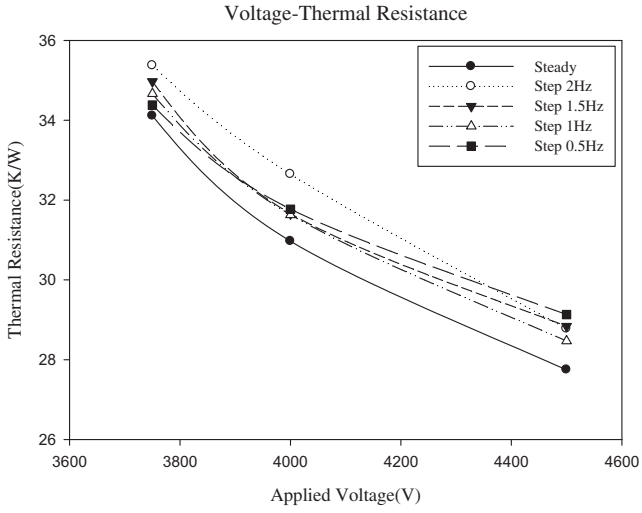

(c) Thermal resistance vs. applied voltage

Fig. 2. Effect of steady and oscillatory EHD on the thermal resistance and the corresponding I–V characteristics for a horizontal separation distance of 5 mm.

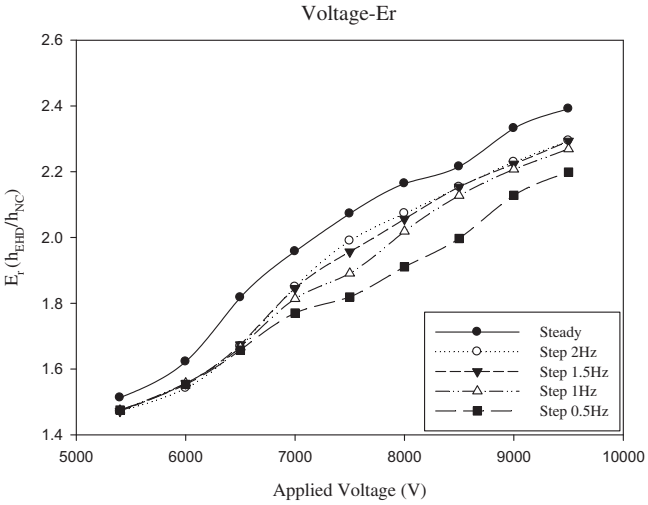

(a) Enhancement index for natural convection vs. applied voltage.

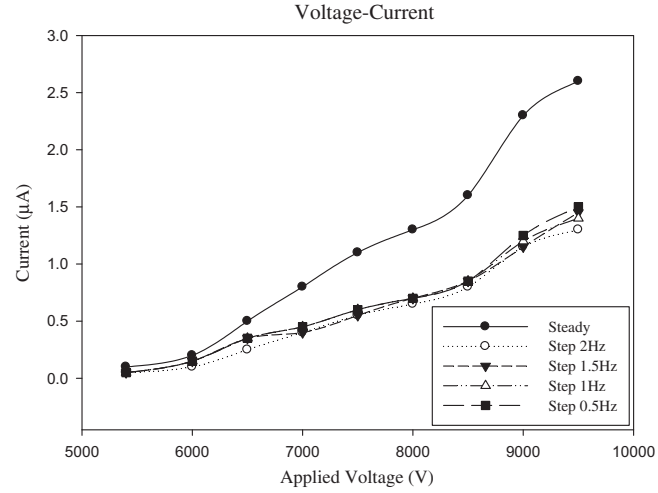

(b) Ionic current vs. applied voltage.

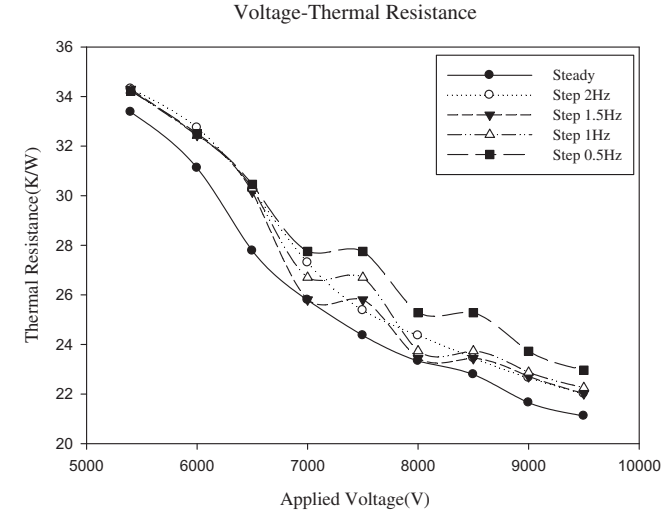

(c) Thermal resistance vs. applied voltage.

Fig. 3. Effect of steady and oscillatory EHD on the thermal resistance and the corresponding I–V characteristics for a horizontal separation distance of 15 mm.

the configuration is different between the current study and theirs, the characterized frequency seems to be in line with each other.

The higher heat transfer performance for the oscillatory EHD at a lower frequency of 0.5 Hz is also indirectly supported by the measured I–V characteristics shown in Fig. 2(b) where the measured

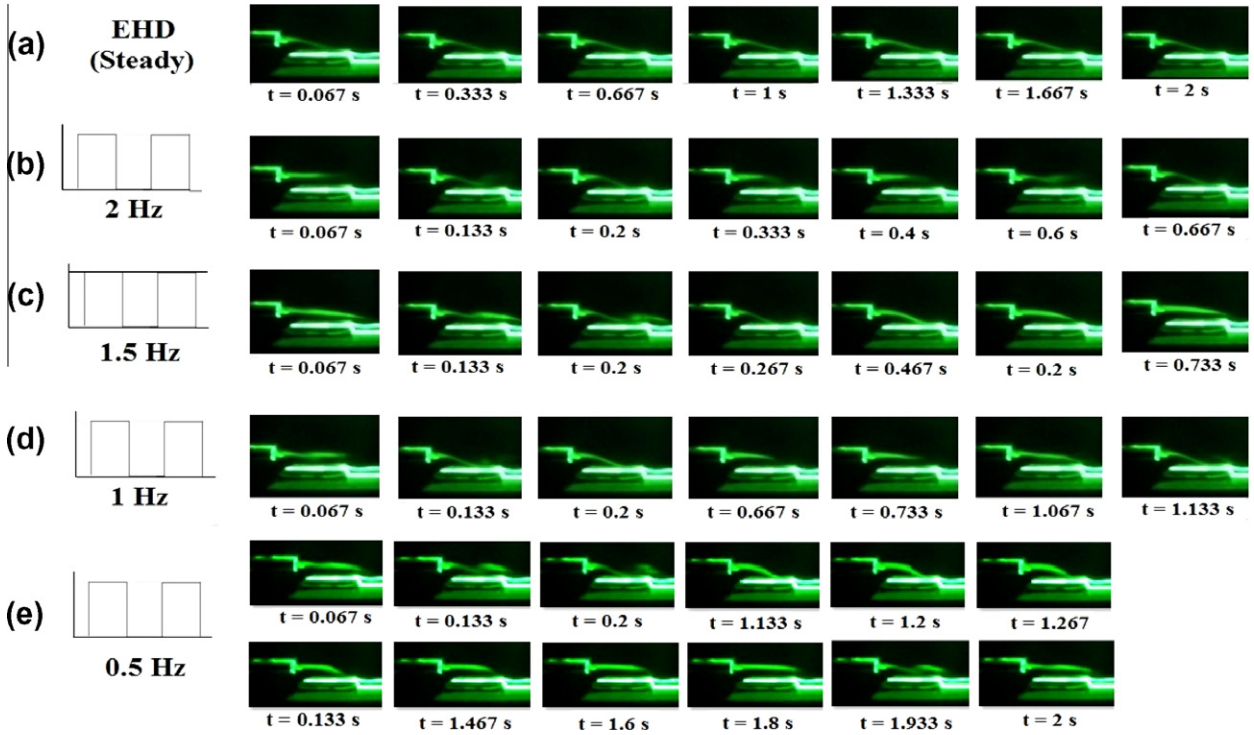

Fig. 4. Progress of observed induced air flow pattern with and without the influence oscillatory EHD.

ionic current for $f = 0.5$ Hz is slightly higher than that of $f = 2$ Hz. Since the induced ionic wind velocity is proportional to the square root of corona current [25], it therefore suggests a higher heat transfer performance at a lower frequency of 0.5 Hz. In the meantime, it is interesting to note that the ionic current for the oscillatory EHD poses a rather linear relation with the applied voltage. Notice that the ionic current for the steady EHD operation is normally proportional to the square of the supplied voltage provided the threshold voltage is exceeded. It is not fully understood why it reveals a rather linear dependence between the ionic current and supplied voltage. One of the possible explanations may be attributed to lesser contribution of the avalanche due to periodic shut-off of the electric field.

Test results for a larger separation distance of 15 mm are depicted in Fig. 3. It is interested to note that the observed enhancement ratio for the oscillatory EHD shows an opposite trend when the horizontal separation distance is increased to 15 mm. Despite the heat transfer performance under oscillatory EHD is still inferior to that of the steady one at the same supplied voltage, the heat transfer performance of the higher frequency ($f = 2$ Hz) exceeds that of the lower frequency ($f = 0.5$ Hz) as shown in Fig. 3(a). Explanations of this result are twofold. Firstly, as pointed out by Baffigi and Bartoli [26] who conducted the heat transfer enhancement study for an inclined plate subject to air pulsating jet. Their results clearly showed that the downstream enhancement is more apparent than that of upstream. Therefore it explains partially about the rise of the heat transfer performance as the separation distance is increased. Note that the spark-over voltage is considerably increased with the separation distance, leading to a considerable rise of enhancement ratio (as high as 2.4 compared to only 1.8 in Fig. 2(a)). Secondly, for a further interpretation of the observed results, it is helpful to examine the associated flow pattern pertaining to the influence of oscillatory EHD. Fig 4 represents the progress of the flow patterns amid various frequencies and that without EHD at a larger separation distance of 15 mm. Notice that the experiment is conducted without heat addition. With a steady EHD input, as shown in Fig. 4(a), the generated smoke is headed toward the test plate. On the other hand, with stepped oscillations of the supplied voltage, the induced airflow does not respond in phase with the oscillatory frequency. As clearly seen in Fig. 4(b), a swinging motion is clearly seen where the smoke first moves toward the test plate and stick close to the plate for some time which is similar to that of a steady EHD operation, and eventually the airflow departs from the surface and again shows a parallel airflow as that without EHD. The oscillatory EHD thus characterizes a swinging flow pattern. The effective time, denoting the time for the directed airflow rested upon the test plate before it departs and swings back to be in parallel with the test plate, for $f = 2$ Hz is longer than that of $f = 0.5$ Hz. For instance, at a smaller frequency like 0.5 Hz, the effective time for the induced airflow toward the test plate is only around 1.1 s in its two seconds operation as shown in Fig. 4(e). Conversely, the effective time for the induced airflow toward the test plate is about 1.4 s over its 2 s operation time when the frequency is raised to 2 Hz. In addition, the swinging motion for $f = 2$ Hz is faster than that $f = 0.5$ Hz. These observations can be easily seen in Fig. 4(b)–(e). As a consequence, the observed results suggested a longer encountered time for the induced airflow alongside the test plate, thereby a higher heat transfer performance is seen for $f = 2$ Hz when compared with that of $f = 0.5$ Hz.

5. Conclusions

This study examines the influence of oscillatory EHD on the heat transfer performance of a flat plate with applied voltage being ranged from 4 to 9.5 kV. The frequency ranges from 0.5 to 2 Hz and the separation distance between the electrode and the test plate is 5 and 15 mm, respectively. Based on the foregoing discussions, the following conclusions are reached:

1. For the same applied voltage, it appears that the heat transfer performance subject to an oscillatory EHD is inferior to that of a steady EHD for all the tested frequencies.

2. A parabolic dependence of the ionic current with the supplied voltage is seen under a steady EHD operation. However, the ionic current vs. supplied voltage shows a rather linear dependence pertaining to an oscillatory EHD input.
3. For a smaller separation distance of 5 mm, the heat transfer performance for $f = 0.5$ Hz is slightly higher than that of $f = 2$ Hz. However, the trend is reversed when the separation distance is increased to 15 mm. This is due to a significant difference in the induced airflow pattern and the effective time rested on the test plate caused by the oscillatory EHD.

Acknowledgment

This work is supported by the National Science Council of Taiwan under contract of 100-2221-E-007-083 and 100-2622-E-009-005-CC2.

References

[1] R. O'brien, A. Shine, Some effects of an electric field on heat transfer from a vertical plate in free convection, J. Heat Transfer 89 (1969) 114–116.
[2] M.E. Franke, Effect of vortices induced by corona discharge on free-convection heat transfer from a vertical plate, J. Heat Transfer 91 (1969) 427–433.
[3] P.H.G. Allen, T.G. Karayiannis, Electrohydrodynamic enhancement of heat transfer and fluid flow, Heat Recovery Syst. CHP 15 (1995) 389–423.
[4] J.C. Shyu, K.W. Hsu, K.S. Yang, C.C. Wang, Thermal characterization of shrouded plate fin array on an LED backlight panel, Appl. Therm. Eng. 31 (2012) 2909–2915.
[5] R.T. Huang, W.J. Sheu, C.C. Wang, Effect of orientation on the natural convective performance of square pin fin heat sinks, Int. J. Heat Mass Transfer 51 (2008) 2368–2376.
[6] S.H. Yu, K.S. Lee, S.J. Yook, Optimum design of a radial heat sink under natural convection, Int. J. Heat Mass Transfer 54 (2011) 2499–2505.
[7] Y. Lai, N. Cordero, F. Barthel, F. Tebbe, J. Kuhn, R. Apfelbeck, D. Wurtenberger, Liquid cooling of bright LEDs for automotive applications, Appl. Therm. Eng. 29 (2009) 1239–1244.
[8] Y. Deng, J. Liu, A liquid metal cooling system for the thermal management of high power LEDs, Int. Commun. Heat Mass Transfer 37 (2010) 788–791.
[9] Z.M. Wan, J. Liu, K.L. Su, X.H. Hu, S.S. M, Flow and heat transfer in porous micro heat sink for thermal management of high power LEDs, Microelectronics 42 (2011) 632–637.
[10] J. Li, B. Ma, R. Wang, L. Han, Study on a cooling system based on thermoelectric cooler for thermal management of high-power LEDs, Microelectron. Reliab. 51 (2011) 2210–2215.
[11] S.M. Marco, H.R. Velkoff, Effect of electrostatic fields on free convection heat transfer from flat plate, ASME Paper, no. 63, ht. 9, 1963.
[12] K. Kibler, H. Carter, Electrocooling in gases, J. Appl. Phys. 45 (1974) 4436–4440.
[13] M. Franke, L. Hogue, Electrostatic cooling of a horizontal cylinder, J. Heat Transfer 113 (1991) 544–548.
[14] M. Ohadi, D. Nelson, S. Zia, Heat transfer enhancement of laminar and turbulent pipe flow via corona discharge, Int. J. Heat Mass Transfer 34 (1991) 1175–1187.
[15] B. Owsenek, J. Seyed-Yagoobi, R. Page, Experimental investigation of corona wind heat transfer enhancement with a heated horizontal flat plate, J. Heat Transfer 117 (1995) 309–315.
[16] B. Owsenek, J. Seyed-Yagoobi, Theoretical and experimental study of electrohydrodynamic heat transfer enhancement through wire-plate corona discharge, J. Heat Transfer 119 (1997) 604–610.
[17] S. Bhattacharyya, A. Peterson, Corona wind-augmented natural convection. Part 1: Single electrode studies, J. Enhanced Heat Transfer 9 (2002) 209–219.
[18] L. Zhao, K. Adamiak, EHD flow in air produced by electric corona discharge in pin–plate configuration, J. Electrostat. 63 (2005) 337–350.
[19] R.T. Huang, W.J. Sheu, C.C. Wang, Heat transfer enhancement by needle-arrayed electrodes – an EHD integrated cooling system, Energy Convers. Manage. 50 (2009) 1789–1796.
[20] D.B. Go, S.V. Garimella, T.S. Fisher, R.K. Mongia, Ionic winds for locally enhanced cooling, J. Appl. Phys. 102 (2007). 053302-053302-8.
[21] D.B. Go, R.A. Maturana, T.S. Fisher, S.V. Garimella, Enhancement of external forced convection by ionic wind, Int. J. Heat Mass Transfer 51 (2008) 6047–6053.
[22] I.Y. Chen, M.Z. Kuo, K.S. Yang, C.C. Wang, Enhanced cooling for LED lighting using ionic wind, Int. J. Heat Mass Transfer 56 (2013) 285–291.
[23] S.J. Kline, F.A. McClintock, Describing the uncertainties in single sample experiments, Mech. Eng. 75 (1953) 3–8.
[24] F.C. Lai, P.J. Mckinney, J.H. Davidson, Oscillatory electrohydrodynamic gas flow, J. Fluids Eng. 117 (1995) 491–497.
[25] M. Robinson, Movement of air in the electric wind of the corona discharge, Trans. AIEE 80 (1961) 143–150.
[26] F. Baffigi, C. Bartoli, Heat transfer enhancement in natural convection between vertical and downward inclined wall and air by pulsating jets, Exp. Therm. Fluid Sci. 34 (2010) 943–953.